



Temperature-driven vapor pressure deficit structures forest

bryophyte communities across the landscapes

- 3 Anna Růžičková ^{1,2}, Matěj Man ^{1,2}, Martin Macek ¹, Jan Wild ¹, Martin Kopecký ¹
- 4 Institute of Botany of the Czech Academy of Sciences, Zámek 1, Průhonice, CZ-252 43, Czech Republic,
- 5 Department of Botany, Faculty of Science, Charles University, Benátská 2, Prague 2, CZ-128 00, Czech Republic
- 6 Correspondence to: Anna Růžičková (anna.ruzickova @ibot.cas.cz)

7 Abstract

- 8 Atmospheric vapor pressure deficit (VPD) controls local plant physiology and global vegetation productivity.
- 9 However, at ecologically crucial intermediate spatial scales, the processes controlling VPD variability and the role
- of this variability in forest bryophyte community assembly are little known.
- 11 To disentangle processes controlling landscape-scale VPD variability and explore VPD effects on bryophyte
- 12 community composition and richness, we recorded bryophyte communities and simultaneously measured forest
- 13 microclimate air temperature and relative humidity across topographically diverse landscape representing
- 14 bryophyte diversity hotspot in temperate Europe. Based on VPD importance for plant physiology, we hypothesize
- 15 that VPD can be an important also for bryophyte community assembly and that VPD variability will be jointly
- 16 driven by saturated and actual vapor pressure across the topographically diverse landscape with contrasting forest
- 17 types and steep microclimatic gradients.
- 18 Contrary to our expectation, VPD variability in the forest understory was dictated by temperature-driven
- 19 differences in saturated vapor pressure, while actual vapor pressure was surprisingly constant across the landscape.
- 20 Gradients in bryophyte community composition and species richness followed closely the VPD variability. While
- 21 mesic forest bryophytes occurred along the whole VPD gradient, azonally occurring and rare species preferred
- 22 sites with low VPD. In result, low VPD sites represent species-rich microrefugia within the landscape and host
- 23 regionally abundant mesic bryophytes simultaneously with rare species near their distributional range limits.
- 24 Our results showed that VPD variability at ecologically crucial landscape scales is controlled by saturated vapor
- 25 pressure and consequently by the maximum air temperature. Future climate warming will thus increase
- 26 evaporative stress and reshuffle VPD-sensitive forest bryophyte communities even in topographically diverse
- 27 landscapes, which are traditionally considered as microclimatic refugia. Azonally occurring rare bryophyte species
- 28 concentrated in low VPD sites will be especially vulnerable to the future changes in atmospheric VPD.

1. Introduction

29

- 30 Atmospheric vapor pressure deficit (VPD) is a key driver of plant functioning in terrestrial ecosystems (Grossiord
- 31 et al., 2020; Ruehr et al., 2014). Higher VPD means higher evaporative stress for plants, which leads to reduced
- 32 photosynthesis in the short term and drought-induced mortality in the long term (McDowell et al., 2008; Fu et al.,
- 33 2022). Ongoing climate changes further exacerbate this evaporative stress because higher temperatures lead to an
- 34 exponential increase in VPD (Lawrence, 2005; Grossiord et al., 2020). Increasing atmospheric VPD already limits





35 global vegetation productivity (Yuan et al., 2019; López et al., 2021; Lu et al., 2022) and triggers large-scale forest 36 diebacks (Breshears et al., 2013; Eamus et al., 2013; Williams et al., 2013). 37 In contrast to VPD effects on local plant physiology and global vegetation functioning, the understanding of 38 the processes that control landscape-scale VPD variability and the effects of this variability on plant community 39 assembly is limited (Novick et al., 2024). Yet this knowledge is crucial for more realistic predictions of climate 40 change impacts on vegetation and the identification of microclimatic refugia (Ashcroft and Gollan, 2013; Davis et 41 al., 2019; Finocchiaro et al., 2024; Ogée et al., 2024). VPD variability across space reflects the complex interplay 42 between spatial patterns in saturated and actual vapor pressures. While saturated vapor pressure (Psat) is controlled 43 solely by air temperature, actual vapor pressure (Pair) is influenced by many processes operating at different spatial 44 scales ranging from regional atmospheric circulation and precipitation to local evaporation from soil and water 45 surfaces and plant transpiration (Campbell and Norman, 1998). Yet how these contrasting processes integrate into the resulting VPD variability over the landscape is still unknown. 46 47 A deeper understanding of the mechanisms behind landscape-scale VPD variability is particularly important for 48 climate change biology. Scientists predict a temperature increase of up to 4.4 °C by 2100 (IPCC, 2023), which 49 would lead to a more than 40 % increase in VPD for the same atmospheric water vapor content (Will et al., 2013). These changes can also modify VPD variability over the landscape and therefore potentially change 50 51 the distribution of individual species and alter the composition of plant communities. However, VPD effects 52 on plant distribution and community assembly over the landscape are not sufficiently known. 53 Among plants, bryophytes are exceptionally sensitive to evaporative stress because they lack roots, lignified 54 water-conducting system, water storage tissues, and active stomata and have a large surface area in proportion to 55 biomass (Rice et al., 2001, Goffinet and Shaw, 2009). Bryophytes transport water passively, mainly through 56 external capillary spaces between tiny parts of their body (Schofield, 1981), and their internal water content is thus 57 a function of the water availability in the surrounding environment (Vanderpoorten and Goffinet, 2009). When 58 this water evaporates, bryophytes can survive in a desiccated state (Proctor, 2000, 2001). Despite this unique 59 bryophyte ability to tolerate desiccation, bryophyte assemblages are potentially highly sensitive to evaporative 60 stress, because desiccation tolerance widely differs among bryophyte species (Hinshiri and Proctor, 1971; Wagner and Titus, 1984, Oliver et al., 2000; Proctor, Ligrone, et al., 2007; Proctor, Oliver, et al., 2007). Yet surprisingly 61 62 little is known about the VPD effect on bryophyte assemblages in temperate forests (Fenton and Frego, 2005). 63 Here we combine detailed in-situ forest microclimate measurements with simultaneous bryophyte inventories

2. Material and methods

68 2.1 Study area

64

65

66

67

We recorded bryophytes and measured microclimate in the Bohemian Switzerland National Park in the Czech Republic (Fig. 1). The rugged terrain of this sandstone landscape creates a fine-scale mosaic of contrasting habitats

to provide this missing knowledge. Specifically, we quantified VPD variability over the topographically diverse

landscape, identified which processes drive this variability, and explored how landscape-scale VPD variability

affects bryophyte community composition and species richness in temperate forests.

- 71 with steep microclimatic gradients over short distances (Wild et al., 2013). The elevation within the national park
- 72 ranges from 125 to 619 m and the mean elevation is 340 m. According to the data from the Tokáň weather station





73 (Fig. 1), the mean annual air temperature during the 2011-2019 period was 8.3 °C, and the mean annual precipitation was 765 mm.

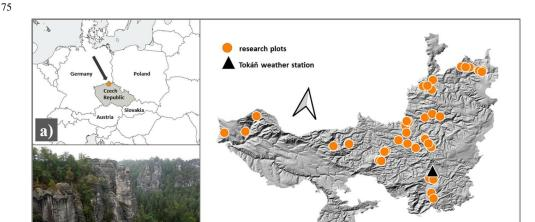


Figure 1: We measured microclimate and simultaneously recorded bryophyte species composition at 38 permanent research plots within the Bohemian Switzerland National Park in Central Europe (a). This forested area has rugged terrain creating steep environmental gradients over short distances (b). The location of the 38 research plots and the Tokáň weather station within the area of the national park (c).

Most of the Bohemian Switzerland is covered with coniferous forests. Historically planted Norway spruce (*Picea abies*) predominates in the valleys and on the plateaus, while patches of semi-natural forests are dominated either by Scots pine (*Pinus sylvestris*) on the upper slopes and rocky ridges or by European beech (*Fagus sylvatica*) on more mesic sites.

The nutrient-poor and strongly acidic soils result in a relatively low diversity of vascular plants, which contrasts with the rich bryophyte flora (Härtel et al., 2007). With more than 300 bryophyte species, the Bohemian Switzerland is a hotspot of bryophyte diversity in Central Europe (Marková, 2008).

The bryophyte flora of the Bohemian Switzerland is dominated by species like *Tetraphis pellucida*, *Bazzania trilobata*, and *Dicranum scoparium*. These dominant floristic elements are enriched by azonal occurrences of (sub)alpine or (sub)montane (e.g., *Hygrobiella laxifolia*, *Geocalyx graveolens*, *Anastrophyllum michauxii*), boreal (e.g., *Dicranum majus*, *Rhytidiadelphus subpinnatus*) and (sub)oceanic (e.g., *Tetrodontium brownianum*, *Plagiothecium undulatum*) species (Härtel et al., 2007; Marková, 2008).

2.2 Field data collection

We recorded bryophyte species composition and measured microclimate on 38 permanent plots within the Bohemian Switzerland National Park (Fig. 1). These plots were selected through stratified-random sampling to capture the main microclimatic gradients within the core zone of the national park. Within each permanent plot, we installed HOBO U23 ProV2 (Onset, USA) microclimatic datalogger protected by a white radiation shield with good ventilation and placed at 1.5 m height on the north side of a tree nearest to the plot center. Each HOBO datalogger measured air temperature (resolution 0.02 °C, accuracy \pm 0.21 °C) and relative humidity (resolution 0.05 %, accuracy \pm 2.5 %) every 30 minutes from 1 June to 31 August 2022.





- Simultaneously with microclimate measurements, we recorded the presence of all bryophyte species in each research plot following the nomenclature of the Czech national checklist (Kučera et al., 2012). We deliberately sampled bryophytes in a relatively small area (3.14 m²) to reduce the possible effects of within-plot environmental
- heterogeneity (Rambo and Muir, 1998; Vanderpoorten and Engels, 2002; Schmalholz and Hylander, 2011).

2.3 Microclimate data processing

- 106 First, we checked the microclimatic time series using visual inspection and standard automated procedures
- 107 implemented in the myClim R package (Man et al., 2023). Using checked air temperature and relative humidity
- data, we calculated the saturated vapor pressure (P_{sat}) following the updated Buck formula (Buck, 1981, 1996):
- $109 \qquad P_{sat} = \ (1.003 + 4.18 \times 10^{-6} \times 101 \ kPa) \times 0.61115 \times e^{((23.036 t/333.7)*(t/(279.82 + t)))},$
- 110 where t is air temperature [°C].
- 111 Then, we calculated the actual vapor pressure (Pair) using the Tetens's formula (Tetens, 1930):
- 112 $P_{air} = P_{sat} \times \left(\frac{rh}{100}\right)$,
- where *rh* is relative humidity [%].
- Finally, we calculated atmospheric VPD as the difference between P_{sat} and P_{air} (Jones, 2014).
- 115 From the resulting time series, we extracted plot-specific daily maximum VPD and Psat and Pair values at the time
- of daily maximum VPD (Tab. 1).
- Table 1: Summary statistics of microclimatic variables measured in 38 forest research plots during summer (June-August 2022). Vapor pressure deficit is the average daily maximum, while saturated and actual vapor pressure are averages of these variables at the time of maximum daily VPD.

	Abbreviation	Mean across all plots	Range of plot means
Saturated vapor pressure	P_{sat}	4.00 kPa	2.61–5.02 kPa
Actual vapor pressure	P_{air}	1.90 kPa	1.75–2.08 kPa
Vapor pressure deficit	VPD	2.09 kPa	0.62-3.17 kPa

2.4 Data analysis

120

121

128

2.4.1 Spatial VPD variability

- 122 To quantify spatial variability in daily VPD, P_{sat} and P_{air}, we calculated the standard deviation (SD) of the daily
- $123 \qquad \text{maximum VPD and corresponding P_{sat} and P_{air} values and averaged these daily SD values over the study period as}$
- an overall measure of spatial variability for each microclimatic variable.
- 125 To disentangle the contribution of P_{sat} and P_{air} to the VPD variability, we performed variation partitioning
- 126 (Legendre, 2008) based on a multiple linear regression model with the average daily maximum VPD as the
- 127 response variable and the average daily values of P_{sat} and P_{air} at the time of daily maximum VPD as the predictors.

2.4.2 Bryophyte communities

- 129 We explored the relationship between atmospheric VPD and bryophyte communities through three steps. First, we
- 130 quantified the VPD link to species richness, then, we explored the VPD, P_{sat}, and P_{air} relationship to main gradients
- in community composition and finally, we directly tested VPD effects on species composition.





- 132 To quantify the relationship between the VPD and species richness expressed as a number of bryophyte species 133 recorded in the plot, we used a generalized additive model (GAM) fitted with the R package mgcv 1.9.1 (Wood, 134 2011). We used GAM with Poisson distribution, log link function, and smooth terms fitted by thin plate regression splines without null space penalization and smoothing parameter estimation using restricted maximum likelihood. 135 136 To explore the main gradients in the bryophyte community composition, we used non-metric multidimensional 137 scaling (NMDS) based on the Sørensen dissimilarity. We calculated two-dimensional NMDS with the weak 138 treatment of ties, a maximum of 500 random starts, and 999 iterations in each NMDS run using metaMDS function 139 from the vegan R package version 2.6-4 (Oksanen et al., 2022). To maximize variance along the first ordination 140 axis, we centered and rotated the resulting two-dimensional configuration with principal component analysis. 141 To explore whether main compositional gradients correlate with microclimate variables, we passively projected 142 gradients in VPD, P_{sat} and P_{air} into the NMDS ordination space and tested the significance of the fit with 999 143 random permutations using the envfit function from vegan R package (Oksanen et al., 2022). Finally, we projected bryophyte species richness gradients into the NMDS ordination space using a generalized additive model fitted 144 145 through ordisurf function from vegan R package (Oksanen et al., 2022). 146 To directly test the effect of the average daily maximum VPD on bryophyte species composition, we used distance-147 based redundancy analysis (db-RDA) (McArdle and Anderson, 2001). As a response variable, we used two 148 community dissimilarity matrices, each reflecting different aspects of community composition. First, we used 149 a community dissimilarity matrix based on the Sørensen index, which expresses differences in species composition including differences in species richness. Second, we used the Simpson index, which expresses species turnover 150 151 independent of the species richness differences (Lennon et al., 2001). To assess the statistical significance of the 152 VPD effect, we used a permutation test with 999 random permutations (Legendre et al., 2011). 153 We used R version 4.4.0 (R Core Team 2024) for complete data analysis and figure preparation. For the colour 154 scheme of Fig. 2 and Fig. 4, we used the R package scico 1.5.0 (Pedersen and Crameri, 2023).
- 155 **3. Results**
- 156 **3.1 VPD variability**
- 157 VPD in the forest understory was highly variable across the landscape, Fig. 2. The VPD values measured every
- 158 30 minutes during summer months ranged from 0 kPa to 8.83 kPa with an overall mean of 0.85 kPa. The overall
- 159 average daily maximum VPD was 2.09 kPa and ranged from 0.62 to 3.17 kPa among the plots (Tab. 1
- and Appendix A, Fig. A1 a Fig. A2).





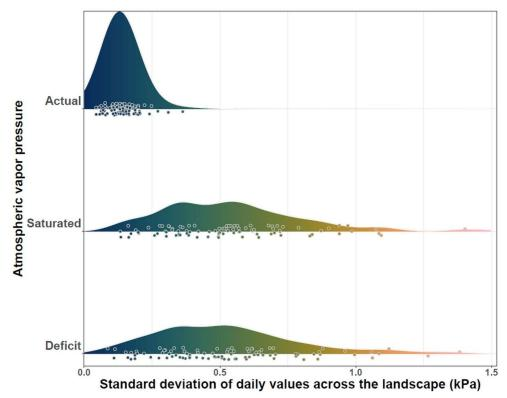
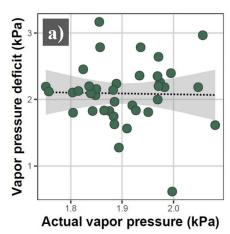


Figure 2: Spatial variability of VPD and its components – saturated and actual atmospheric vapor pressures. Each data point shows the standard deviation of the daily values simultaneously measured at 38 forest plots, and density plots summarize this spatial variability over the summer season. The individual data points were slightly jittered for better visibility.

The spatial variability of P_{sat} (average daily SD = 0.55 kPa) was almost four times higher than the spatial variability of P_{air} (SD = 0.14 kPa). Saturated vapor pressure was also the dominant driver of the VPD variability across the landscape (Fig. 3) because P_{sat} explained 97 % of VPD variability, while P_{air} explained only 3 %.







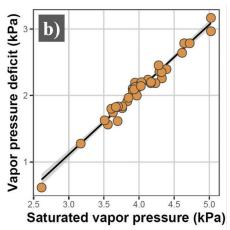


Figure 3: Atmospheric vapor pressure deficit (VPD) at 38 forest plots sampled over topographically diverse landscape was dictated by temperature-dependent saturated vapor pressure (b), while actual vapor pressure was not related to local VPD (a). Each dot represents the average daily maximum VPD and the corresponding average saturated and actual vapor pressure during the summer season.

3.2 Bryophyte communities

In total, we recorded 39 bryophyte species: 14 liverworts and 25 mosses (Appendix C, Tab. C1). The average number of species per plot was 8, minimum 1 and maximum 21. The most frequent species were *Dicranum scoparium*, *Leucobryum juniperoideum* and *Hypnum cupressiforme*.

Main patterns in community composition and species richness reflected VPD variability (Fig. 4). While the gradients in VPD and P_{sat} were significantly related to the main patterns in community composition (VPD: $R^2 = 0.37$, p = 0.001; P_{sat} : $R^2 = 0.34$, p = 0.001), the gradient in P_{air} was not ($R^2 = 0.09$, p = 0.17). The number of bryophyte species was higher in plots with low VPD and declined with increasing VPD (GAM: explained deviance $D^2 = 31.2 \%$, $\chi^2 = 23.37$, p = 0.0008).





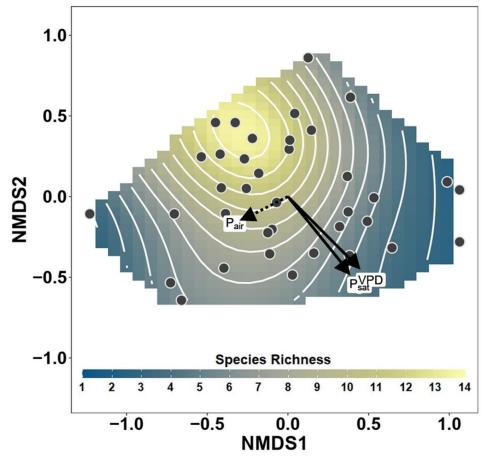


Figure 4: Nonmetric multidimensional scaling (NMDS) of the bryophyte community composition shoving main gradients in bryophyte assemblages sampled at 38 temperate forest plots. Points show the positions of the individual plots within the NMDS ordination space, and the vectors show the gradients in the average daily maximum VPD and corresponding saturated and actual vapor pressures. The smooth surface and associated contours show the pattern in species richness (number of species per plot) fitted into the NMDS ordination space with a generalized additive model.

Atmospheric VPD was a significant predictor of the community composition of forest bryophytes. The average daily maximum VPD explained 10.95 % of the variation in species composition expressed with the Sørensen index (pseudo-F = 4.43, p = 0.001) and 13.52 % of the variation in species composition expressed with the Simpson index (pseudo-F = 5.63, p = 0.004).

Small liverworts (e.g. Riccardia multifida, Lophozia ventricosa) and hygrophilous bryophytes (e.g. Polytrichum commune, Bazzania trilobata), as well as boreal (e.g. Dicranum majus) and (sub)oceanic (e.g. Mylia taylorii, Plagiothecium undulatum) species preferred plots with low atmospheric VPD (Fig. 5). In contrast, mesic species like Hypnum cupressiforme, Polytrichum formosum or Dicranum scoparium occurred also in plots with higher atmospheric VPD.





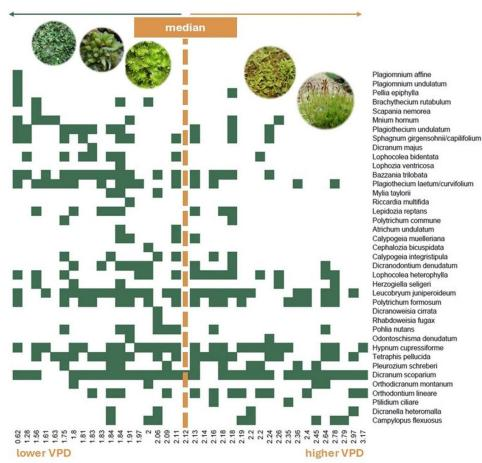


Figure 5: Occurrences of all recorded bryophyte species along the gradient of the average daily maximum VPD measured at 38 forest plots. Plots are sorted from the lowest to highest VPD and each filled square shows the presence of the focal species within the plot. While rare and azonally occurring species prefer sites with low VPD, mesic species occur along the whole VPD gradient.

4. Discussion

Our findings have important implications both for theoretical and applied ecology. First, the variation in VPD over the landscape was controlled by maximum air temperature. Therefore, these two microclimatic variables are tightly coupled at biologically relevant scales, and their effects are hard to disentangle with observational data. Maximum temperatures were identified as a key driver of bryophyte and vascular plant species distribution in temperate forests (Macek et al., 2019; Man et al., 2022). Unfortunately, these studies did not measure VPD. Considering our results, the importance of maximum temperature does not necessarily stem from its direct effects on plant ecophysiology, but more likely from strong temperature control of VPD variability over the landscape. Nevertheless, this new hypothesis needs further testing.

Second, our results imply that it is possible to estimate VPD from local microclimate air temperature measurements combined with non-local measurements of air relative humidity, for example from a nearby weather station. While the general applicability of this approach should be further tested in various environmental settings and across





- different vegetation types, our findings suggest that local VPD can be reasonably estimated (Appendix B, Fig. B1).
- This finding thus opens exciting possibilities for further research as local temperature measurements are
- increasingly available all over the world (Lembrechts et al., 2020).

4.1 VPD variability across the landscape

- 217 Large spatial variability in atmospheric VPD structured forest bryophyte communities across the landscape.
- 218 Interestingly, VPD variation was driven by temperature-controlled P_{sat}, while P_{act} was relatively constant across
- the landscape. This finding is important, as the actual vapor pressure should also be variable across the landscape
- 220 (Johnston et al., 2025, Ogeé et al. 2024). However, our findings suggest that the local and spatially highly
- 221 heterogeneous processes like evaporation from soil and water surfaces and plant transpiration do not contribute
- much to the landscape-scale variation in VPD.
- 223 Microclimate variation over the landscape, crucial for community ecology, is largely dictated by land-surface
- 224 topography (Dobrowski, 2011). Land-surface topography controls also maximum air temperatures in the forest
- 225 understory (Macek et al., 2019) and therefore spatial variability in saturation vapor pressure. However, we were
- 226 surprised that the highly localized processes like evapotranspiration did not contribute much to the spatial
- 227 variability in absolute air humidity despite our study area with extremely rugged topography and contrasting forest
- 228 vegetation types. Therefore, spatial variability in absolute air humidity seems to be determined mostly by processes
- 229 operating at much larger scales like atmospheric circulation and precipitation patterns (Campbell and Norman,
- 230 1998).

238

- 231 Given the growing recognition of VPD importance for many ecosystem processes, plant distribution, and
- 232 community assembly (Grossiord et al., 2020; Kopecký et al., 2024; Novick et al., 2024), the approach we
- 233 developed here to disentangle the contribution of saturated versus actual vapor pressure can provide new insights
- 234 into the drivers of VPD variability across spatial and temporal scales. So far, the knowledge of the relative
- 235 importance of saturated versus actual vapor pressure is limited, therefore it is difficult to compare our results with
- 236 other studies. Nevertheless, a comparison of the drivers of VPD variability across agricultural fields in Germany
- 237 supports our conclusion (Wörlen et al., 1999).

4.2 VPD effects on bryophytes

- 239 Bryophytes inevitably lose water when exposed to the air with non-zero VPD (Hinshiri and Proctor, 1971; Busby
- 240 and Whitfield, 1978). At full turgor, bryophyte cells have osmotic potential rarely more negative than -2 MPa
- 241 (Proctor, 2000). An osmotic potential of -1.36 MPa is in equilibrium with air at 20 °C and 99% relative humidity
- 242 (i.e. VPD < 0.03 kPa). If the temperature remains at 20 °C, but the relative humidity drops to 90 %, the water
- $243 \qquad \text{potential outside the bryophyte body decreases to -14 MPa (Proctor, 2000) and bryophytes start to lose water. To} \\$
- maintain full turgor and normal cell function, bryophytes thus need free liquid water close to the cells. However,
- this external water completely evaporates within 45-50 minutes if atmospheric VPD reaches 1.22 kPa (León-
- Vargas et al., 2006). Once the external water evaporates, bryophyte cells rapidly lose turgor, metabolic activity
- 247 slows down, and carbon fixation decreases. In our study region, such favorable conditions without evaporative
- stress and VPD lower than 0.03 kPa occurred only 9 % of the measurement time.
- 249 In contrast to vascular plants, bryophytes tolerate desiccation and become metabolically inactive in the absence of
- 250 water (Proctor, 2000). When conditions improve, bryophytes quickly reactivate physiological processes such as

https://doi.org/10.5194/egusphere-2025-1244 Preprint. Discussion started: 10 April 2025 © Author(s) 2025. CC BY 4.0 License.



268



251 respiration, photosynthesis, cell cycle, or normal cytoskeleton function (Proctor, Ligrone, et al., 2007; Proctor, 252 Oliver, et al., 2007). However, this reactivation requires a lot of energy, for example to produce specific repair 253 proteins (Oliver and Bewley, 1984; Zeng et al., 2002) or to maintain the integrity and normal function of cell 254 organelles and membranes (Platt et al., 1994). Prolonged periods without evaporative stress are therefore key for 255 bryophyte growth and long-term survival (Proctor, Oliver, et al., 2007). 256 Large VPD variability over the landscape creates fine-scaled mosaic of sites with widely different evaporative 257 stress and this environmental template structured bryophyte communities. Regionally rare species preferred sites 258 with low VPD. These species – otherwise typical for (sub)montane, boreal, or (sub)oceanic regions – are 259 approaching their distributional limits within our study area (Hill and Preston, 1998). For these species, sites with 260 low VPD serve as microclimatic refugia within an otherwise unsuitable landscape matrix. In contrast, widespread 261 mesic bryophytes occurred along the whole VPD gradient. Sites with low atmospheric VPD, hosting 262 simultaneously rare as well as widespread bryophytes, thus represent hotspots of bryophyte diversity in the 263 landscape. 264 With climate warming, areas with low VPD will likely shrink, and their bryophyte diversity will become more 265 vulnerable (Pardow and Lakatos, 2013). Moreover, the increasingly frequent and severe canopy disturbances will likely increase understory temperatures and therefore also VPD (Wolf et al., 2021; Máliš et al., 2023). Our results 266 267 suggest that such changes will reshuffle bryophyte communities, supporting widespread mesic bryophytes at the

expense of regionally rare species near their distributional limits.

269 4.3 Disentangling atmospheric VPD and temperature 270 The close coupling between VPD and maximum temperature across the landscape clearly shows the need - and 271 simultaneously the difficulty - of disentangling the influences of VPD and temperature on plant communities. 272 While temperature affects basic life functions of bryophytes like photosynthesis, respiration (Dilks and Proctor, 273 1975), and growth (Furness and Grime, 1982), bryophytes thrive in a wide range of temperatures - from less than 274 -30 °C (Dilks and Proctor, 1975) to over 40 °C in a dry state (Hearnshaw and Proctor, 1982). For most bryophytes, 275 the optimal growth temperature ranges from 12 to 25 °C (Vanderpoorten and Goffinet, 2009). However, many 276 bryophyte species grow even at temperatures around 5 °C (Dilks and Proctor, 1975), and some can even 277 photosynthesize at temperatures below 0 °C (Lösch et al., 1983). Therefore, temperature is hardly a direct limiting 278 factor of bryophyte distribution and community composition in temperate regions. 279 Several studies of vascular plants have attempted to distinguish the independent effect of VPD from other 280 microclimatic factors affecting plant functioning and distribution (Eamus et al., 2013; Denham et al., 2021; Flo et 281 al., 2022; Fu et al., 2022; Kopecký et al., 2024), highlighting the critical importance of VPD (Novick et al., 2016; 282 Schönbeck et al., 2022). Unfortunately, no physiological studies addressed the independent effects of VPD 283 on bryophytes, despite clear indications that VPD plays a key role (Busby et al., 1978; Sonnleitner et al., 2009). 284 So far, studies of bryophyte physiology concentrated on desiccation tolerance (Morales-Sánchez et al., 2022). 285 While desiccation tolerance is an adaptation to cope with the external lack of water, the ultimate driver of 286 desiccation is atmospheric VPD. A deeper focus on atmospheric VPD can therefore bring a new insight into 287 bryophyte ecology and distribution.





5. Conclusions

Atmospheric VPD controls community composition and richness of bryophyte assemblages in temperate forest understory. Even across the landscape with extremely rugged terrain, spatial variability in atmospheric VPD was controlled by temperature-dependent saturated vapor pressure. Maximum air temperature and VPD are thus tightly coupled at biologically relevant scales and their effects are hard to disentangle. Nevertheless, both ecological and physiological studies suggest that bryophytes in temperate zone are not directly limited by temperature (Dilks and Proctor, 1975; Furness and Grime, 1982) but rather by evaporative stress represented by VPD (Busby et al., 1978; Dilks and Proctor, 1979). With climate warming, the tight coupling between VPD and local air temperature will cause nonlinear increases in VPD-driven evaporative stress, which will subsequently reshuffle bryophyte community composition and decrease species richness. Especially vulnerable will be azonally occurring bryophyte species concentrated in microclimatic refugia with low VPD.

Appendix A

300 VPD variability over the summer season

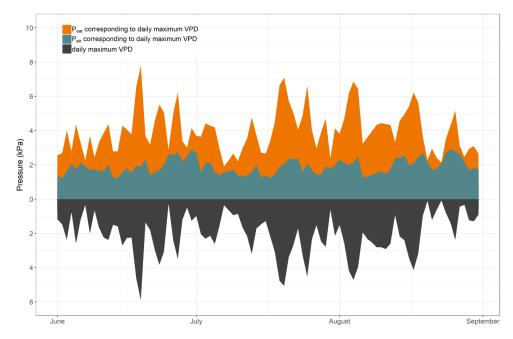
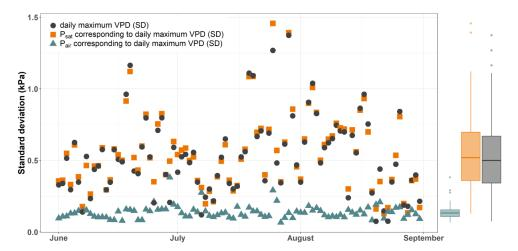


Figure A1: Daily values of maximum vapor pressure deficit (VPD) and corresponding values of saturated (P_{sat}) and actual (P_{air}) vapor pressures, averaged over 38 permanent vegetation plots during June-August 2022.







 $Figure \ A2: Spatial\ variability\ of\ VPD\ (black\ circles)\ is\ tightly\ coupled\ with\ the\ spatial\ variability\ in\ P_{sat}\ (orange\ squares)$ but not with Pair (blue triangles). Each data point shows the standard deviation of the daily value measured at 38 study sites. Marginal boxplots summarize spatial variability (daily standard deviations) during the growing season (June-August 2022).

Appendix B

303

304

305

306

307

308

309

310

311

312

313

314

315

316

317 318

319

VPD estimate from in-situ air temperature and regional air humidity

Based on our results, we speculated that local atmospheric VPD can be reasonably estimated using the in-situ air temperature measurements paired with relative air humidity measurements representative for the whole region (and therefore the same for all plots situated within that region). To explore this idea, we estimated the average daily maximum atmospheric VPD using in-situ measured air temperature (HOBO U23 ProV2 dataloggers in 1.5 m height) and relative air humidity measured in the Tokáň weather station located in the study area (Fig. 1). While the measured and estimated VPD were closely correlated (Pearson r = 0.98), estimated VPD tended to be higher than in-situ measured VPD (Fig. B1). Therefore, we conclude that the relative position of the site on the VPD gradient can be reasonably estimated from

in-situ microclimate temperature measurements paired with regional relative air humidity measurements. However, this approach does not provide a reliable estimate of local atmospheric VPD, especially on sites with locally higher air humidity.

320

321



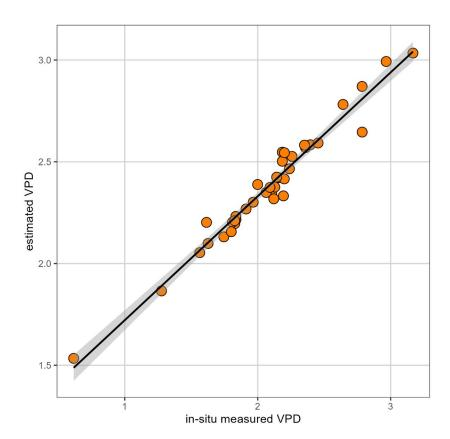


Figure B1: Relationship between in-situ measured average daily maximum VPD and average daily maximum VPD estimated from in-situ measured air temperature and relative air humidity measured in regional weather station (June-August 2022). While the measured and estimated VPD are closely correlated (Pearson r=0.98), estimated VPD tends to be higher than in-situ measured VPD, likely because of locally higher air humidity in topographically sheltered sites near valley bottoms.

Appendix C

322

323 324 325

326

327

329

330

328 List of bryophyte species, their occurrence and biogeographical affinity

Table C1: Complete species list of bryophyte species recorded at 38 study plots. Biogeographical categories follow Hill and Preston (1998).

	Species name	Occurence	Taxonomic group	Major biome	Eastern limit
1	Dicranum scoparium	32	moss	Wide-boreal	Circumpolar
2	Leucobryum juniperoideum	26	moss	Temperate	European
3	Hypnum cupressiforme	24	moss	Wide-temperate	Circumpolar
4	Tetraphis pellucida	21	moss	Boreo-temperate	Circumpolar
5	Bazzania trilobata	18	liverwort	Temperate	Suboceanic





6	Polytrichum formosum	17	moss	Boreo-temperate	Circumpolar
7	Lophocolea heterophylla	15	liverwort	Temperate	Circumpolar
8	Plagiothecium laetum/curvifolium	15	moss	Boreal- montane/Temperate	Circumpolar/European
9	Orthodontium lineare	13	moss	Temperate	European
10	Plagiothecium undulatum	11	moss	Boreo-temperate	Suboceanic
11	Pleurozium schreberi	10	moss	Boreo-temperate	Circumpolar
12	Sphagnum girgensohnii/capillifolium	10	moss	Boreo-arctic Montane/Boreo- temperate	Circumpolar
13	Dicranodontium denudatum	9	moss	Boreal-montane	European
14	Campylopus flexuosus	8	moss	Temperate	Suboceanic
15	Lepidozia reptans	8	liverwort	Boreo-temperate	Circumpolar
16	Lophocolea bidentata	8	liverwort	Temperate	European
17	Pohlia nutans	8	moss	Wide-boreal	Circumpolar
18	Mnium hornum	7	moss	Temperate	European
19	Calypogeia integristipula	6	liverwort	Boreo-temperate	Circumpolar
20	Herzogiella seligeri	5	moss	Boreo-temperate	European
21	Brachythecium rutabulum	4	moss	Temperate	European
22	Calypogeia mulleriana	4	liverwort	Boreo-temperate	Circumpolar
23	Dicranella heteromalla	4	moss	Boreo-temperate	Circumpolar
24	Orthodicranum montanum	4	moss	Boreo-temperate	Circumpolar
25	Mylia taylorii	3	liverwort	Boreal-montane	Suboceanic
26	Atrichum undulatum	2	moss	Boreo-temperate	Circumpolar
27	Dicranum majus	2	moss	Boreo-temperate	Circumpolar
28	Odontoschisma denudatum	2	liverwort	Boreo-temperate	European
29	Pellia epiphylla	2	liverwort	Boreo-temperate	Circumpolar
30	Polytrichum commune	2	moss	Wide-boreal	Circumpolar
31	Ptilidium ciliare	2	liverwort	Boreo-arctic Montane	Circumpolar
32	Cephalozia bicuspidata	1	liverwort	Boreo-temperate	Circumpolar
33	Dicranoweisia cirrata	1	moss	Temperate	European
34	Lophozia ventricosa	1	liverwort	Boreo-temperate	European
35	Plagiomnium affine	1	moss	Temperate	European
36	Plagiomnium undulatum	1	moss	Temperate	European
37	Rhabdoweisia fugax	1	moss	Boreal-montane	European
38	Riccardia multifida	1	liverwort	Boreo-temperate	Circumpolar
39	Scapania nemorea	1	liverwort	Boreo-temperate	European

Data availability. The data supporting the findings of this study are currently provided for peer review on GitHub

public repository (https://doi.org/10.5281/zenodo.14989898).





333 Author contribution. Conceptualization: AR, MMan, MMac, JW, MK. Funding acquisition: MK. Data curation: 334 AR. Methodology: MMac, MK. Formal analysis: AR. Investigation: AR, MMan, MMac, JW, MK. Visualization: 335 AR, MMan, MMac, MK. Writing - original draft: AR. Writing - review & editing: AR, MMan, MMac, JW, MK. 336 Supervision: MK. 337 Competing interest. The authors declare that they have no conflict of interest. 338 Acknowledgements. We thank all colleagues who helped us to collect microclimate data. We also thank the Administration of the Bohemian Switzerland National Park for their long-term support. 339 340 Financial support. This study was supported by the Czech Science Foundation (project GACR 23-06614S) and 341 the Czech Academy of Sciences (project RVO 67985939). 342 References 343 Ashcroft, M. B. and Gollan, J. R.: Moisture, thermal inertia, and the spatial distributions of near-surface soil 344 and air temperatures: understanding factors that promote microrefugia, Agr. Forest Meteorol., 345 176, 77-89, https://doi.org/10.1016/j.agrformet.2013.03.008, 2013. 346 Breshears, D. D., Adams, H. D., Eamus, D., McDowell, N. G., Law, D. J., Will, R. E., Williams, A. P., and 347 Zou, C. B.: The critical amplifying role of increasing atmospheric moisture demand on tree 348 mortality and associated regional die-off, Front. Plant Sci., 4, 2-5, https://doi.org/10.3389/fpls.2013.00266, 2013. 349 350 Buck, A. L.: New equations for computing vapor pressure and enhancement factor. J. Appl. Meteorol. Clim., 20(12), 1527–1532, https://doi.org/10.1175/1520-0450(1981)020<1527:NEFCVP>2.0.CO;2, 351 352 1981. 353 Buck, A. L.: Buck research manual, 1996. 354 Busby, J. R., Bliss, L. C., and Hamilton, C. D.: Microclimate control of growth rates and habitats of the boreal 355 forest mosses, Tomenthypnum nitens and Hylocomium splendens, Ecol. Monogr., 48(2), 95-110, https://doi.org/10.2307/2937294, 1978. 356 357 Busby, J. R. and Whitfield, D. W. A.: Water potential, water content, and net assimilation of some boreal forest mosses, Can. J. Botany, 56(13), 1551–1558, https://doi.org/10.1139/b78-184, 1978. 358 359 Campbell, G. S. and Norman, J. M.: An introduction to environmental biophysics, 2nd ed., Springer, New York, 286 pp., https://doi.org/10.1007/978-1-4612-1626-1, 1998. 360 361 Davis, K. T., Dobrowski, S. Z., Holden, Z. A., Higuera, P. E., and Abatzoglou, J. T.: Microclimatic buffering 362 in forests of the future: the role of local water balance, Ecography, 42(1), 1–11, https://doi.org/10.1111/ecog.03836, 2019. 363 Denham, S. O., Oishi, A. C., Miniat, C. F., Wood, J. D., Yi, K., Benson, M. C., and Novick, K. A.: Eastern US 364 365 deciduous tree species respond dissimilarly to declining soil moisture but similarly to rising evaporative demand, Tree Physiol., 41(6), 1-56, https://doi.org/10.1093/treephys/tpaa153, 2021. 366 367 Dilks, T. J. K. and Proctor, M. C. F: Comparative experiments on temperature responses of bryophytes: assimilation, respiration and freezing damage, J. Bryol., 8(3), 317-336, 368 369 https://doi.org/10.1179/jbr.1975.8.3.317, 1975.







370	Dilks, T. J. K. and Proctor, M. C. F.: Photosynthesis, respiration and water content in bryophytes, New
371	Phytol., 82(1), 97–114, https://doi.org/10.1111/j.1469-8137.1979.tb07564.x, 1979.
372	Dobrowski, S. Z.: A climatic basis for microrefugia: the influence of terrain on climate, Global Change Biol.,
373	17(2), 1022–1035, https://doi.org/10.1111/j.1365-2486.2010.02263.x , 2011.
374	Eamus, D., Boulain, N., Cleverly, J., and Breshears, D. D.: Global change-type drought-induced tree
375	mortality: vapor pressure deficit is more important than temperature per se in causing decline in
376	tree health, Ecol. Evol., 3(8), 2711–2729, https://doi.org/10.1002/ece3.664, 2013.
377	Fenton, N. J. and Frego, K. A.: Bryophyte (moss and liverwort) conservation under remnant canopy in
378	managed forests, Biol. Conserv., 122(3), 417–430, https://doi.org/10.1016/j.biocon.2004.09.003,
379	2005.
380	Finocchiaro, M., Médail, F., Saatkamp, A., Diadema, K., Pavon, D., Brousset, L., and Meineri, E.:
381	Microrefugia and microclimate: unraveling decoupling potential and resistance to heatwaves,
382	Sci. Total Environ., 924, 171696, https://doi.org/10.1016/j.scitotenv.2024.171696, 2024.
383	Flo, V., Martínez-Vilalta, J., Granda, V., Mencuccini, M., and Poyatos, R.: Vapour pressure deficit is the main
384	driver of tree canopy conductance across biomes, Agr. Forest Meteorol., 322, 109029,
385	https://doi.org/10.1016/j.agrformet.2022.109029, 2022.
386	Fu, Z., Ciais, P., Prentice, I. C., Gentine, P., Makowski, D., Bastos, A., Luo, X., Green, J. K., Stoy, P. C.,
387	Yang, H., and Hajima, T.: Atmospheric dryness reduces photosynthesis along a large range of
388	soil water deficits, Nat. Commun., 13(1), 1–10, https://doi.org/10.1038/s41467-022-28652-7,
389	2022.
390	Furness, S. B. and Grime, J. P.: Growth rate and temperature responses in bryophytes: II. A comparative study
391	of species of contrasted ecology, J. Ecol., 70(2), 525–536, https://doi.org/10.2307/2259920 ,
392	1982.
393	Goffinet, B. and Shaw, J. A. (Eds.): Bryophyte biology, 2nd ed., Cambridge University Press, New York, 556
394	pp., ISBN 978-0-521-69322-6, 2009.
395	Grossiord, C., Buckley, T. N., Cernusak, L. A., Novick, K. A., Poulter, B., Siegwolf, R. T. W., Sperry, J. S.,
396	and McDowell, N. G.: Plant responses to rising vapor pressure deficit, New Phytol., 226(6),
397	1550–1566, https://doi.org/10.1111/nph.16485 , 2020.
398	Härtel, H., Sádlo, J., Świerkosz, K., and Marková, I.: Phytogeography of the sandstone areas in the Bohemian
399	Cretaceous Basin (Czech Republic/Germany/Poland), in: Sandstone landscapes, edited by:
400	Härtel, H., Cílek, V., Herben, T., Jackson, A., and Williams, R., Academia, Praha, 177-189,
401	https://doi.org/10.6084/m9.figshare.92598, 2007.
402	Hearnshaw, G. F. and Proctor, M. C. F.: The effect of temperature on the survival of dry bryophytes, New
403	Phytol., 90(2), 221–228, https://doi.org/10.1111/j.1469-8137.1982.tb03254.x , 1982.
404	Hill, M. O. and Preston, C. D.: The geographical relationships of British and Irish bryophytes, J. Bryol., 20(1),
405	127–226, https://doi.org/10.1179/jbr.1998.20.1.127, 1998.
406	Hinshiri, H. M. and Proctor, M. C. F.: The effect of desiccation on subsequent assimilation and respiration of
407	the bryophytes Anomodon viticulosus and Porella platyphylla, New Phytol., 70(3), 527-538,
408	https://doi.org/10.1111/j.1469-8137.1971.tb02554.x, 1971.
409	IPCC: Climate Change 2023: synthesis report, https://doi.org/10.59327/IPCC/AR6-9789291691647 , 2023.





410	Johnston, M. R, Barnes, M. L., Preisler, Y., Smith, W. K., Biederman, J. A., Scott, R. L., Williams, A. P., and
411	Dannenberg, M. P.: Effects of hot versus dry vapor pressure deficit on ecosystem carbon and
412	water fluxes, J. Geophys. ResBiogeo., 130(1), e2024JG008146,
413	https://doi.org/10.1029/2024JG008146, 2025.
414	Jones, H. G.: Plants and microclimate: a quantitative approach to environmental plant physiology, 3rd ed.,
415	Cambridge University Press, https://doi.org/10.1017/CBO9780511845727 , 2014.
416	Kopecký, M., Hederová, L., Macek, M., Klinerová, T., and Wild, J.: Forest plant indicator values for moisture
417	reflect atmospheric vapour pressure deficit rather than soil water content, New Phytol., 244(5),
418	1801-1811., https://doi.org/10.1111/nph.20068, 2024.
419	Kučera, J., Váňa, J., and Hradílek. Z.: Bryophyte flora of the Czech Republic: updated checklist and Red List
420	and a brief analysis, Preslia, 84(3), 813–850, 2012.
421	Lawrence, M. G.: The relationship between relative humidity and the dewpoint temperature in moist air: a
422	simple conversion and applications, B. Am. Meteorol. Soc., 86(2), 225-234,
423	https://doi.org/10.1175/BAMS-86-2-225, 2005.
424	Legendre, P.: Studying beta diversity: ecological variation partitioning by multiple regression and canonical
425	analysis, J. Plant Ecol.,1(1), 3–8, https://doi.org/10.1093/jpe/rtm001 , 2008.
426	Legendre, P., Oksanen, J., and ter Braak, C. J. F.: Testing the significance of canonical axes in redundancy
427	analysis, Methods Ecol. Evol., 2(3), 269–277, https://doi.org/10.1111/j.2041-
428	<u>210X.2010.00078.x</u> , 2011.
429	Lembrechts, J. J., Aalto, J., Ashcroft, M. B., et al.: SoilTemp: a global database of near-surface temperature,
430	Glob. Change Biol., 26(11), 6616–6629, https://doi.org/10.1111/gcb.15123 , 2020.
431	Lennon, J. J., Koleff, P., Greenwood, J. J. D., and Gaston, K. J.: The geographical structure of British bird
432	distributions: diversity, spatial turnover and scale, J. Anim. Ecol., 70(6), 966-979,
433	https://doi.org/10.1046/j.0021-8790.2001.00563.x, 2001.
434	León-Vargas, Y., Engwald, S., and Proctor, M. C. F.: Microclimate, light adaptation and desiccation tolerance
435	of epiphytic bryophytes in two Venezuelan cloud forests, J. Biogeogr., 33(5), 901-913,
436	https://doi.org/10.1111/j.1365-2699.2006.01468.x, 2006.
437	López, J., Way, D. A., and Sadok, W.: Systemic effects of rising atmospheric vapor pressure deficit on plant
438	physiology and productivity, Glob. Change Biol., 27(9), 1704-1720,
439	https://doi.org/10.1111/gcb.15548, 2021.
440	Lösch, R., Kappen, L., and Wolf, A.: Productivity and temperature biology of two snowbed bryophytes, Polar
441	Biol., 1(4), 243–248, https://doi.org/10.1007/BF00443195, 1983.
442	Lu, H., Qin, Z., Lin, S., Chen, X., Chen, B., He, B., Wei, J., and Yuan, W.: Large influence of atmospheric
443	vapor pressure deficit on ecosystem production efficiency, Nat. Commun., 13(1), 10-13,
444	https://doi.org/10.1038/s41467-022-29009-w, 2022.
445	Macek, M., Kopecký, M., and Wild, J.: Maximum air temperature controlled by landscape topography affects
446	plant species composition in temperate forests, Landscape Ecol., 34, 2541-2556,
447	https://doi.org/10.1007/s10980-019-00903-x, 2019.





448	Máliš, F., Ujházy, K., Hederová, L., Ujházyová, M., Csölleová, L., Coomes, D. A., and Zellweger, F.:
449	Microclimate variation and recovery time in managed and old-growth temperate forests, Agr.
450	Forest Meteorol., 342, 109722, https://doi.org/10.1016/j.agrformet.2023.109722, 2023.
451	Man, M., Kalčík, V., Macek, M., Brůna, J., Hederová, L., Wild, J., and Kopecký, M.: myClim: microclimate
452	data handling and standardised analyses in R, Methods Ecol. Evol., 14(9), 2308-2320,
453	https://doi.org/10.1111/2041-210X.14192, 2023.
454	Man, M., Wild, J., Macek, M., and Kopecký, M.: Can high-resolution topography and forest canopy structure
455	substitute microclimate measurements? Bryophytes say no., Sci. Total Environ., 821, 153377,
456	https://doi.org/10.1016/j.scitotenv.2022.153377, 2022.
457	Marková, I.: Mechorosty Českého Švýcarska (Labských pískovců), in: Labské pískovce - historie, příroda a
458	ochrana území, edited by: Bauer, P., Kopecký, V., and Šmucar, J., Agentura ochrany přírody
459	a krajiny ČR, Správa CHKO Labské pískovce, Děčín, 106-120, 2008. [in Czech language]
460	McArdle, B. H. and Anderson, M. J.: Fitting multivariate models to community data: a comment on distance-
461	based redundancy analysis, Ecology, 82(1), 290–297, https://doi.org/10.1890/0012-
462	9658(2001)082[0290:FMMTCD]2.0.CO;2, 2001.
463	McDowell, N., Pockman, W. T., Allen, C. D., Breshears, D. D., Cobb, N., Kolb, T., Plaut, J., Sperry, J., West,
464	A., Williams, D. G., and Yepez, E. A.: Mechanisms of plant survival and mortality during
465	drought: why do some plants survive while others succumb to drought?, New Phytol., 178(4),
466	719–739, https://doi.org/10.1111/j.1469-8137.2008.02436.x, 2008.
467	Morales-Sánchez, J. Á. M., Mark, K., Souza, J. P.S., and Niinemets, Ü.: Desiccation – rehydration
468	measurements in bryophytes: current status and future insights, J. Exp. Bot., 73(13), 4338–4361,
469	https://doi.org/10.1093/jxb/erac172, 2022.
470	Novick, K. A., Ficklin, D. L., Grossiord, C., Konings, A. G., Martínez-Vilalta, J., Sadok, W., Trugman, A. T.,
471	Williams, A. P., Wright, A. J., Abatzoglou, J. T., Dannenberg, M. P., Gentine, P., Guan, K.,
472	Johnston, M. R., Lowman, L. E. L., Moore, D. J. P., and McDowell, N. G.: The impacts of
473	rising vapour pressure deficit in natural and managed ecosystems, Plant Cell Environ., 47(9),
474	3561-3589, https://doi.org/10.1111/pce.14846, 2024.
475	Novick, K. A., Ficklin, D. L., Stoy, P. C., Williams, C. A., Bohrer, G., Oishi, A. C., Papuga, S. A., Blanken, P.
476	D., Noormets, A., Sulman, B. N., Scott, R. L., Wang, L., and Phillips, R. P.: The increasing
477	importance of atmospheric demand for ecosystem water and carbon fluxes, Nat. Clim. Change,
478	6(11), 1023–1027, https://doi.org/10.1038/nclimate3114, 2016.
479	Ogée, J., Walbott, M., Barbeta, A., Corcket, E., and Brunet, Y.: Decametric-scale buffering of climate
480	extremes in forest understory within a riparian microrefugia: the key role of microtopography,
481	Int. J. Biometeorol., 68(9), 1741–1755, https://doi.org/10.1007/s00484-024-02702-9, 2024.
482	Oksanen, J., Simpson, G., Blanchet, F., Kindt, R., Legendre, P., Minchin, P. R., O'Hara, R. B., Solymos, P.,
483	Stevens, M. H. H., Szoecs, E., Wagner, H., Barbour, M., Bedward, M., Bolker, B., Borcard, D.,
484	Carvalho, G., Chirico, M., De Caceres, M., Durand, S., Evangelista, H. B. A., FitzJohn, R.,
485	Friendly, M., Furneaux, G., Hill, M. O., Lahti, L., McGlinn, D., Ouellette, M-H., Cunha, E. R.,
486	Smith, T., Stier, A., ter Braak, C. J. F., Weedon, J., and Borman, T.: vegan: Community





487	Ecology Package [R package vegan version 2.6-4], https://cran.r-project.org/package=vegan ,
488	5 Feb. 2025, 2022.
489	Oliver, M. J. and Bewley, J. D.: Plant desiccation and protein synthesis, Plant Physiol., 74(4), 923-927,
490	https://doi.org/10.1104/pp.74.4.923, 1984.
491	Oliver, M. J., Velten, J., and Wood, A. J.: Bryophytes as experimental models for the study of environmental
492	stress tolerance: Tortula ruralis and desiccation-tolerance in mosses, Plant Ecol., 151(1), 73-84
493	https://doi.org/10.1023/A:1026598724487, 2000.
494	Pardow, A. and Lakatos, M.: Desiccation tolerance and global change: implications for tropical bryophytes in
495	lowland forests, Biotropica, 45(1), 27–36, https://doi.org/10.1111/J.1744-7429.2012.00884.X ,
496	2013.
497	Pedersen, T. and Crameri, F.: scico: Colour palettes based on the scientific colour maps [R package scio version
498	1.5.0], https://CRAN.R-project.org/package=scico , 11 Mar. 2025, 2023.
499	Platt, K. A., Oliver, M. J., and Thomson, W. W.: Membranes and organelles of dehydrated Selaginella and
500	Tortula retain their normal configuration and structural integrity: freeze fracture evidence,
501	Protoplasma, 178(1-2), 57-65, https://doi.org/10.1007/BF01404121, 1994.
502	Proctor, M. C. F. The bryophyte paradox: tolerance of dessication, evasion of drought, Plant Ecol., 151(1),
503	41–49, https://doi.org/10.1023/A:1026517920852, 2000.
504	Proctor, M. C. F. Patterns of desiccation tolerance and recovery in bryophytes, Plant Growth Regul., 35(2),
505	147–156, https://doi.org/10.1023/A:1014429720821, 2001.
506	Proctor, M. C. F., Ligrone, R., and Duckett, J. G.: Desiccation tolerance in the moss <i>Polytrichum formosum</i> :
507	physiological and fine-structural changes during desiccation and recovery, Ann. BotLondon,
508	99(1), 75–93, https://doi.org/10.1093/aob/mcl246, 2007.
509	Proctor, M. C. F, Oliver, M. J., Wood, A. J., and Alpert, P.: Desiccation-tolerance in bryophytes: a review,
510	Bryologist, 110(4), 595-621, https://doi.org/10.1639/0007-
511	2745(2007)110[595:DIBAR]2.0.CO;2, 2007.
512	R Core Team: R: A language and environment for statistical computing, R foundation for statistical
513	computing, Vienna, Austria, https://www.R-project.org/ , 15 Mar. 2025, 2024.
514	Rambo, T. R. and Muir, P. S.: Forest floor bryophytes of Pseudotsuga menziesii-Tsuga heterophylla stands in
515	Oregon: influence of substrate and overstory, Bryologist, 101(1), 116-130,
516	https://doi.org/10.2307/3244083, 1998.
517	Rice, S. K., Collins, D., and Anderson, A. M.: Functional significance of variation in bryophyte canopy
518	structure, Am. J. Bot., 88(9), 1568–1576, https://doi.org/10.2307/3558400, 2001.
519	Ruehr, N. K., Law, B. E., Quandt, D., and Williams, M.: Effects of heat and drought on carbon and water
520	dynamics in a regenerating semi-arid pine forest: a combined experimental and modelling
521	approach, Biogeosciences, 11, 4139–4156, https://doi.org/10.5194/bg-11-4139-2014, 2014.
522	Schmalholz, M. and Hylander, K.: Microtopography creates small-scale refugia for boreal forest floor
523	bryophytes during clear-cut logging, Ecography, 34(4), 637-348,
524	https://doi.org/10.1111/j.1600-0587.2010.06652.x, 2011.
525	Schofield, W. B.: Ecological significance of morphological characters in the moss gametophyte, Bryologist,
526	84(2), 149–165, https://doi.org/10.2307/3242819 , 1981.





527	Schönbeck, L. C., Schuler, P., Lehmann, M. M., Mas, E., Mekarni, L., Pivovaroff, A. L., Turberg, P., and
528	Grossiord, C.: Increasing temperature and vapour pressure deficit lead to hydraulic damages in
529	the absence of soil drought, Plant, Cell Environ., 45(11), 3275–3289,
530	https://doi.org/10.1111/pce.14425, 2022.
531	Sonnleitner, M., Dullinger, S., Wanek, W., and Zechmeister, H.: Microclimatic patterns correlate with the
532	distribution of epiphyllous bryophytes in a tropical lowland rain forest in Costa Rica, J. Trop.
533	Ecol., 25(3), 321–330, https://doi.org/10.1017/S0266467409006002, 2009.
534	Tetens, O.: Ueber einige meteorologische Begriffe. Zeitschrift für geophysik, 6, 297-309, 1930. [in German
535	language]
536	Vanderpoorten, A. and Engels, P.: The effects of environmental variation on bryophytes at regional scale,
537	Ecography, 25(5), 513-522, https://doi.org/10.1034/j.1600-0587.2002.250501.x, 2002.
538	Vanderpoorten, A. and Goffinet, B.: Introduction to bryophytes, Cambridge University Press, Cambridge, 303
539	pp., https://doi.org/10.1017/CBO9780511626838, 2009.
540	Wagner, D.J. and Titus, J. E.: Comparative desiccation tolerance of two <i>Sphagnum</i> mosses, Oecologia, 62,
541	182–187, https://doi.org/10.1007/BF00379011, 1984.
542	Wild, J., Macek, M., Kopecký, M., Zmeškalová, J., Hadincová, V., and Trachtová, P.: Temporal and spatial
543	variability of microclimate in sandstone landscape: detailed field measurement, in: Proceedings
544	of the 3rd International Conference on Sandstone Landscapes, Sandstone Landscapes, Diversity,
545	Ecology and Conservation, University of Wroclaw, 220–224, 2013.
546	Will, R. E., Wilson, S. M., Zou, C. B., and Hennessey, T. C.: Increased vapor pressure deficit due to higher
547	temperature leads to greater transpiration and faster mortality during drought for tree seedlings
548	common to the forest-grassland ecotone, New Phytol., 200(2), 366-374,
549	https://doi.org/10.1111/nph.12321, 2013.
550	Williams, A. P., Allen, C. D., Macalady, A. K., Griffin, D., Woodhouse, C. A., Meko, D. M., Swetnam, T. W.,
551	Rauscher, S. A., Seager, R., Grissino-Mayer, H. D., Dean, J. S., Cook, E. R., Gangodagamage,
552	C., Cai, M., and McDowell, N. G.: Temperature as a potent driver of regional forest drought
553	stress and tree mortality, Nat. Clim. Change, 3(3), 292–297,
554	https://doi.org/10.1038/nclimate1693, 2013.
555	Wolf, K. D., Higuera, P. E., Davis, K. T., and Dobrowski, S. Z.: Wildfire impacts on forest microclimate vary
556	with biophysical context, Ecosphere, 12(5), e03467, https://doi.org/10.1002/ecs2.3467, 2021.
557	Wood, S. N.: Fast stable restricted maximum likelihood and marginal likelihood estimation of semiparametric
558	generalized linear models, J. R. Stat. Soc.: Series B (Statistical Methodology), 73(1), 3-36,
559	https://doi.org/10.1111/J.1467-9868.2010.00749.X, 2011.
560	Wörlen, C., Schulz, K., Huwe, B., and Eiden, R.: Spatial extrapolation of agrometeorological variables, Agr.
561	For. Meteorol., 94(3-4), 233-242, https://doi.org/10.1016/S0168-1923(99)00015-5, 1999.
562	Yuan, W., Zheng, Y., Piao, S., Ciais, P., Lombardozzi, D., Wang, Y., Ryu, Y., Chen, G., Dong, W., Hu, Z.,
563	Jain, A. K., Jiang, C., Kato, E., Li, S., Lienert, S., Liu, S., Nabel, J. E. M. S., Qin, Z., Quine, T.,
564	Sitch, S., Smith, W. K., Wang, F., Wu, C., Xiao, Z., and Yang, S.: Increased atmospheric vapor
565	pressure deficit reduces global vegetation growth, Sci. Adv., 5(8), 1-13,
566	https://doi.org/10.1126/sciadv.aax1396, 2019.

https://doi.org/10.5194/egusphere-2025-1244 Preprint. Discussion started: 10 April 2025 © Author(s) 2025. CC BY 4.0 License.





567	Zeng, Q., Chen, X., Wood, A. J.: Two early light-inducible protein (ELIP) cDNAs from the resurrection plant
568	Tortula ruralis are differentially expressed in response to desiccation, rehydration, salinity, and
569	high light, J. Exp. Bot., 53(371), 1197–1205, https://doi.org/10.1093/jexbot/53.371.1197, 2002.